

## Supporting Information

### **Nacre-based carbon nanomeshes for soft ionic actuator with large and rapid deformation**

Xiao Han,<sup>‡ab</sup> Meng Kong,<sup>‡a</sup> Mingjie Li,<sup>\*ab</sup> Xiankai Li,<sup>ab</sup> Weiqing Yang<sup>ac</sup> and Chaoxu Li<sup>\*ab</sup>

<sup>a</sup>Group of Biomimetic Smart Materials, Qingdao Institute of Bioenergy and Bioprocess

Technology, Chinese Academy of Sciences, Songling Road 189, Qingdao 266101, P. R.

China.

<sup>b</sup>Center of Material and Optoelectronics Engineering, University of Chinese Academy of

Sciences, 19A Yuquan Road, Beijing 100049, P. R. China.

<sup>c</sup>State Key Laboratory of Bio-fibers and Eco-textiles, Shandong Collaborative Innovation

Center of Marine Biobased Fibers and Ecological textiles, College of Materials Science and

Engineering, Institute of Marine Biobased Materials, Qingdao University, Qingdao 266071,

China

<sup>‡</sup>These authors contributed equally to this work.

\*E-mail: licx@qibebt.ac.cn (C. Li); limj@qibebt.ac.cn (M. Li).

17 **Supporting Table**

18 **Table S1**

Electrode Materials	Voltage (V)	Strain (%)	Power consumption (mW cm <sup>-2</sup> )	Reference
Carbon nanomeshes/PVDF	3	1.11	205.7	This work
Platinum	3	0.32	3981.1	Ref. 54
SWNT	5	0.16	546.43	Ref. 47
PPy	5	0.15	1500.6	Ref. 52
SWNT	2.5	0.29	150.15	Ref. 46
BP-CNT	2.5	1.37	53.29	Ref. 49
BP-CNT	2.5	1.02	41.84	Ref. 49
RGO/MWCNT	2	0.27	53.16	Ref. 20
SWNT	2	0.10	7936.8	Ref. 48
SWNT	2	0.016	3645.5	Ref. 53
RGO/Ag	1	0.45	42.99	Ref. 19
SWCNT	1	1.26	159.79	Ref. 45
PANI@CNT	1	0.24	737.17	Ref. 50
GO/PANI	1	0.45	796.61	Ref. 51
Th-SNG/PEDOT:PSS	0.5	0.2	–	Ref. 10
HPNC/PEDOT:PSS	0.5	0.54	–	Ref. 55
Graphene/Nafion	0.5	0.03	–	Ref. 56

19

20

21

22

23

24

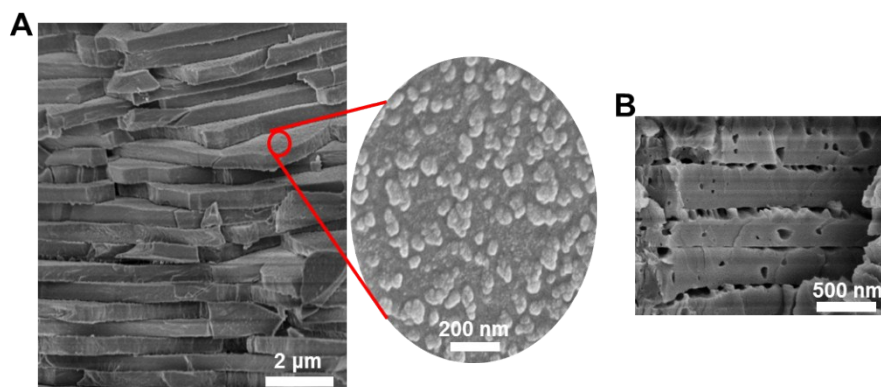
25

26

27

28

29 **Supporting figures**



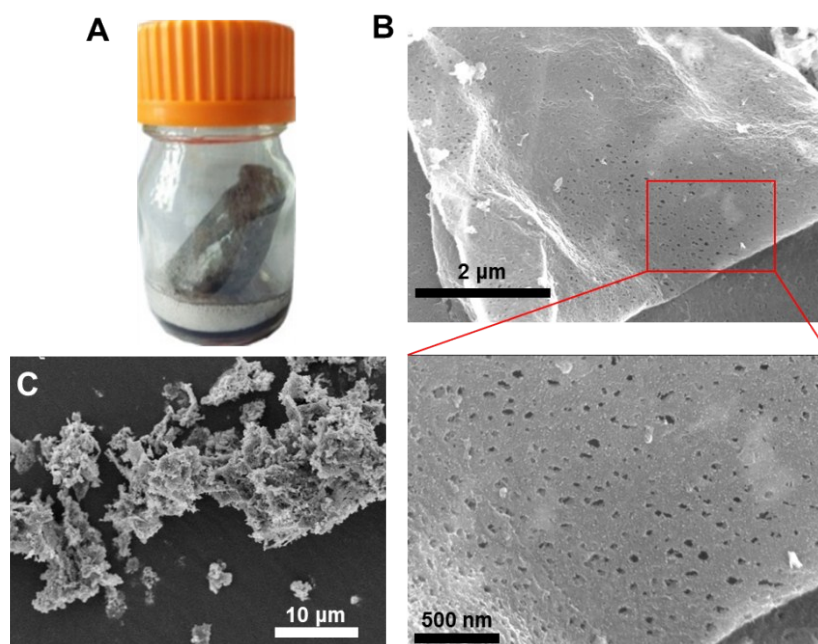
30

31

**Fig. S1** Microstructures of nacre and mineral bridges.

32

33



34

35 **Fig. S2** Synthesis of carbon nanomeshes with Pathway I. (A) Optical image of calcinated

36 nacre in acid solution. (B) SEM of carbon nanomeshes produced at 550 °C. (C) SEM of

37 carbon residues after calcination at 700 °C.



38

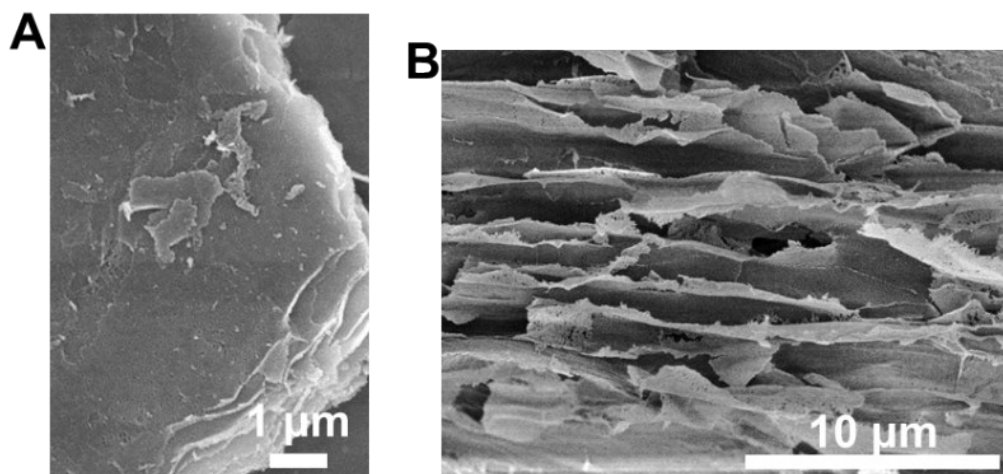
39

**Fig. S3** Thermal degeneration of  $\text{CaCO}_3$  and  $\text{CO}_2$  etching.

40

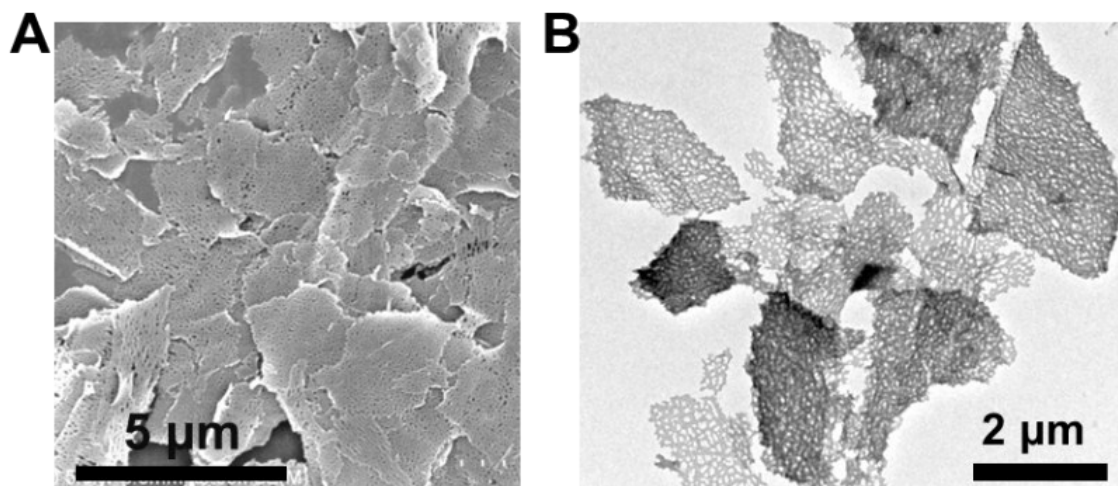
41

42



43

44 **Fig. S4** SEM images of nacre after removing mineral with acids.



45

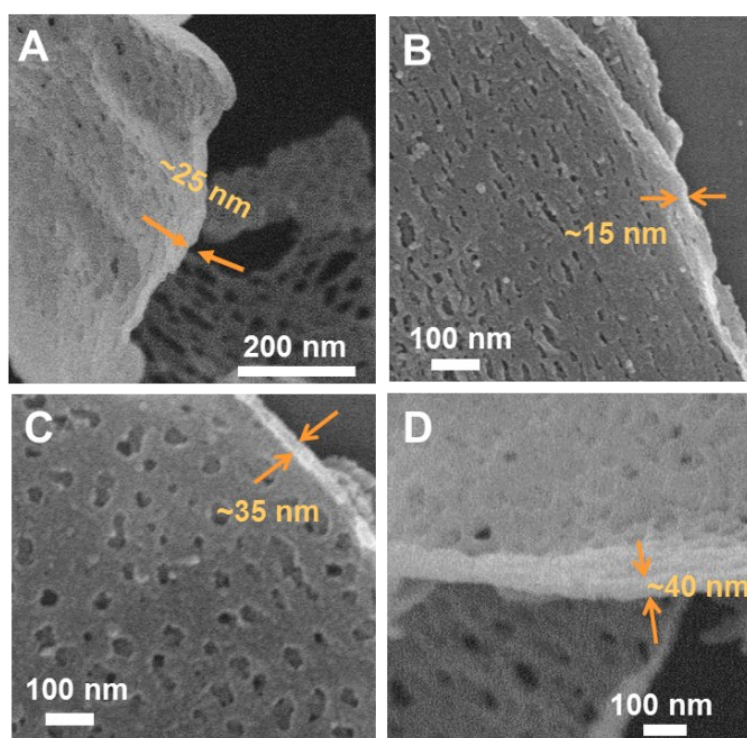
46

**Fig. S5** SEM (A) and TEM (B) images of exfoliated organic nanomeshes.

47

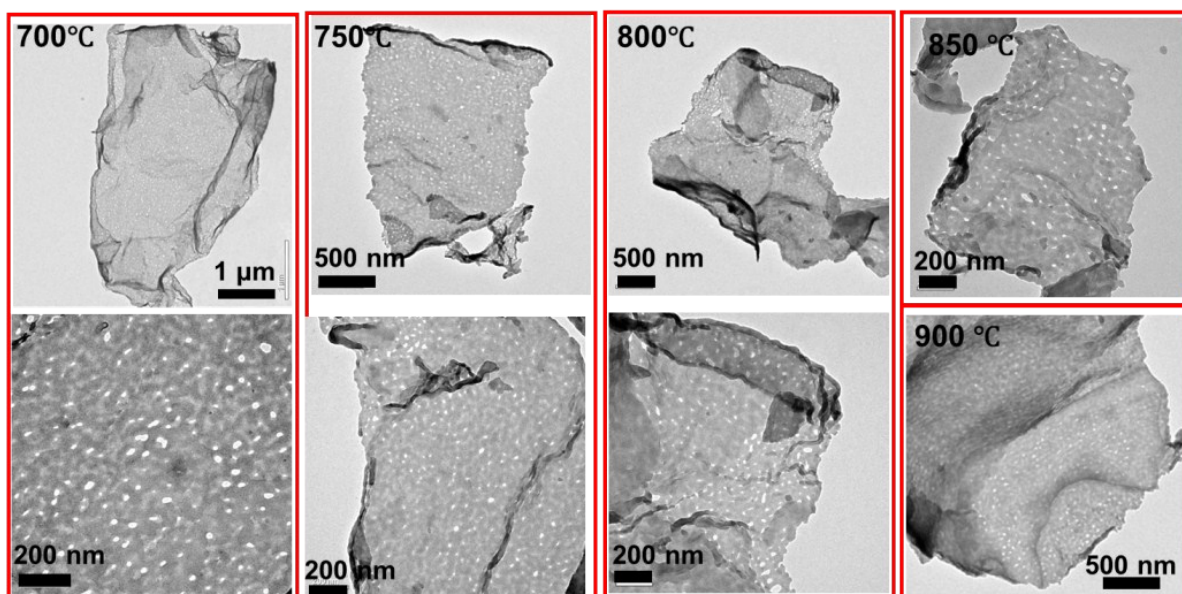
48

49



50

51 **Fig. S6** Typical SEM images of organic nanomeshes, indicating a thickness of ~15–40 nm.



52

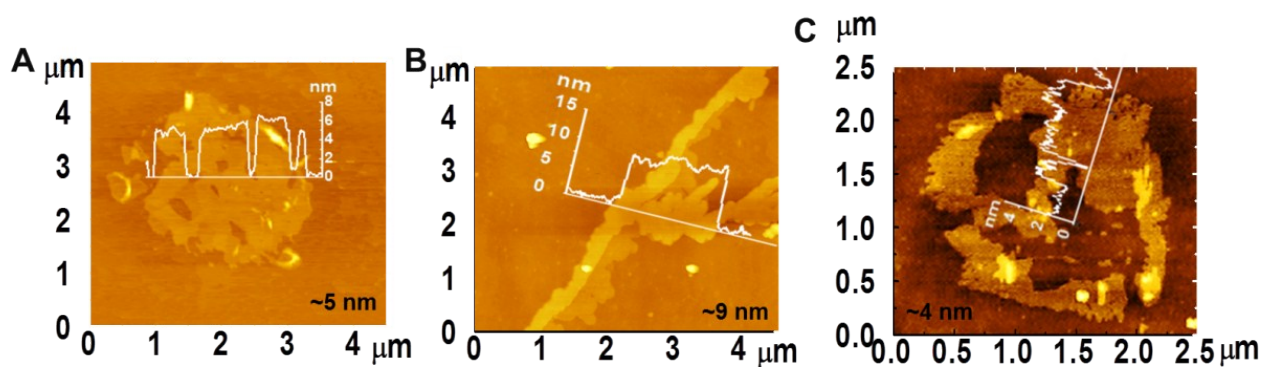
53 **Fig. S7** Typical TEM images of carbon nanomeshes prepared at carbonization temperatures

54 from 700 to 900 °C.

55

56

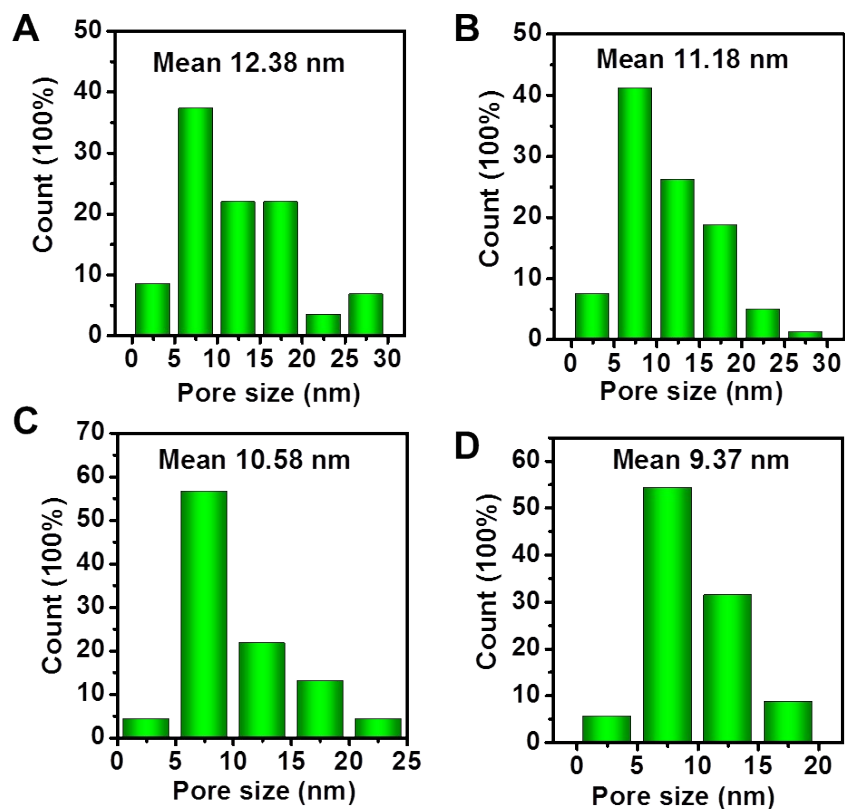
57



58

59 **Fig. S8** Typical height AFM images of carbon nanomeshes prepared at 850 °C and profiles

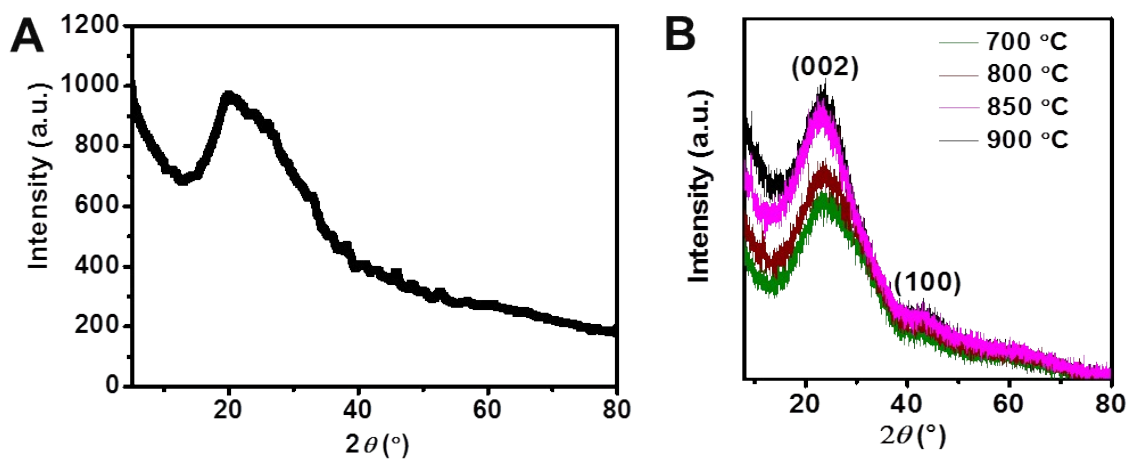
60 along the indicated line. A thickness of ~4–9 nm was observed.



61

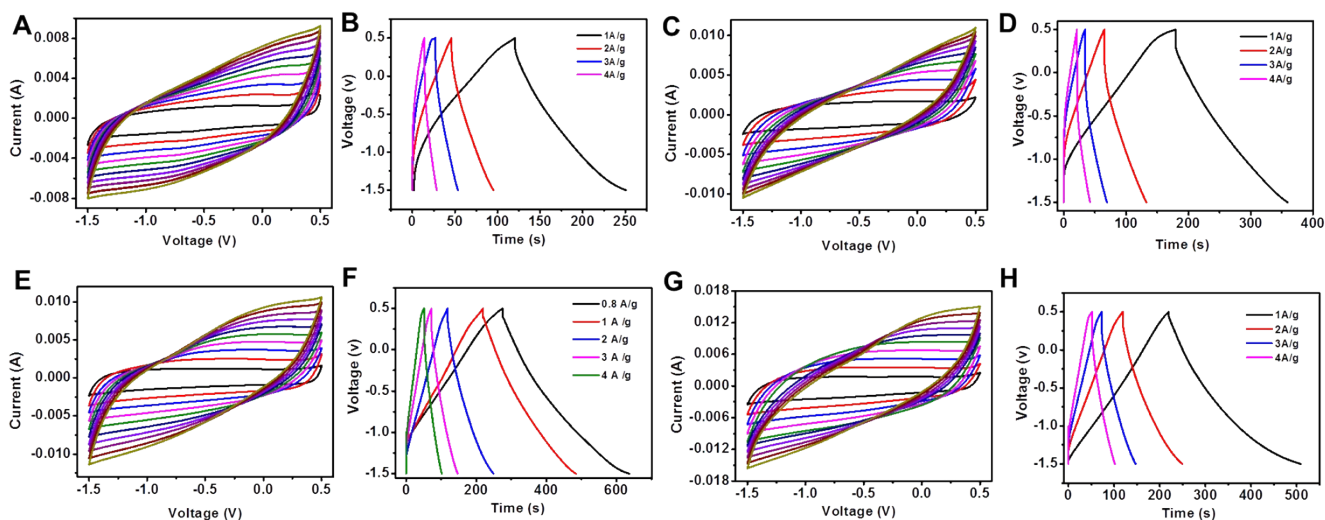
62 **Fig. S9** Histogram of in-plane pore diameters of carbon nanomeshes prepared at temperatures  
 63 of 700 (A), 800 (B), 850 (C) and 900 °C (D).

64



65

66 **Fig. S10** XRD spectra of organic nanosheets (A) and carbon nanomeshes (B) produced at  
 67 different temperatures.



68

69 **Fig. S11** (A, C, E & G) CV curves at different scan rates from 10 to 100  $\text{mV s}^{-1}$  of carbon

70 nanomeshes prepared at temperature of 700 (A), 800 (C), 850 (E) and 900 °C (G). (B, D, F &

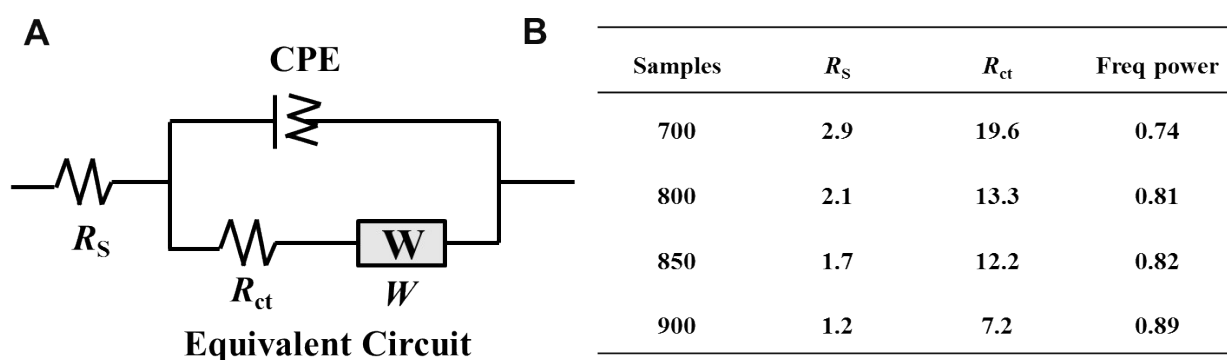
71 H) galvanostatic charge/discharge curves at different current densities from 0.8 to 4  $\text{A g}^{-1}$  of

72 carbon nanomeshes prepared at temperature of 700 (B), 800 (D), 850 (F) and 900 °C (H).

73

74

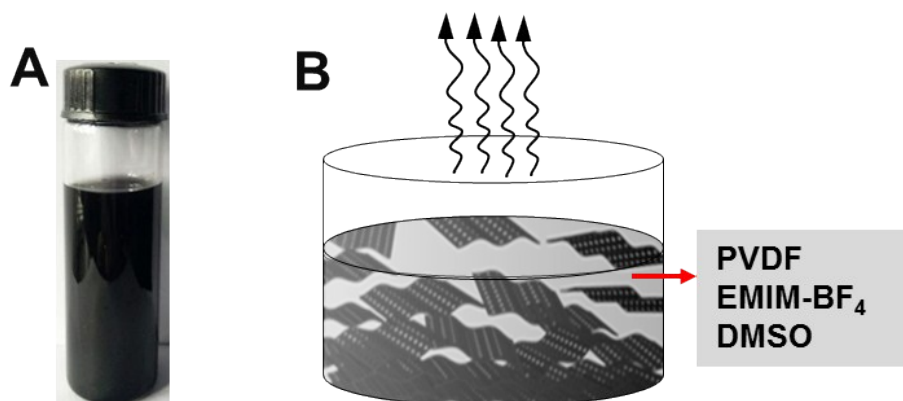
75



76

77 **Fig. S12** Equivalent circuit of Nyquist plots (A) and fitting results (B) of carbon nanomeshes

78 prepared with different calcination temperatures.



79

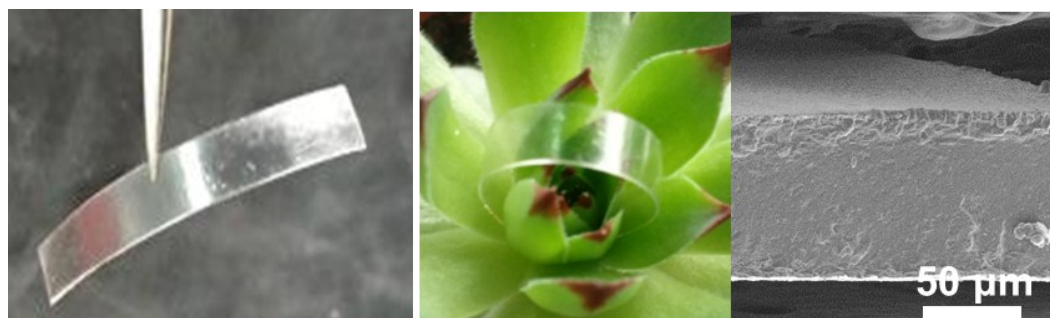
80 **Fig. S13** (A) Optical image of carbon nanomesh dispersion in PVDF. (B) Schematic

81 fabrication of gradient membrane electrode with casting method.

82

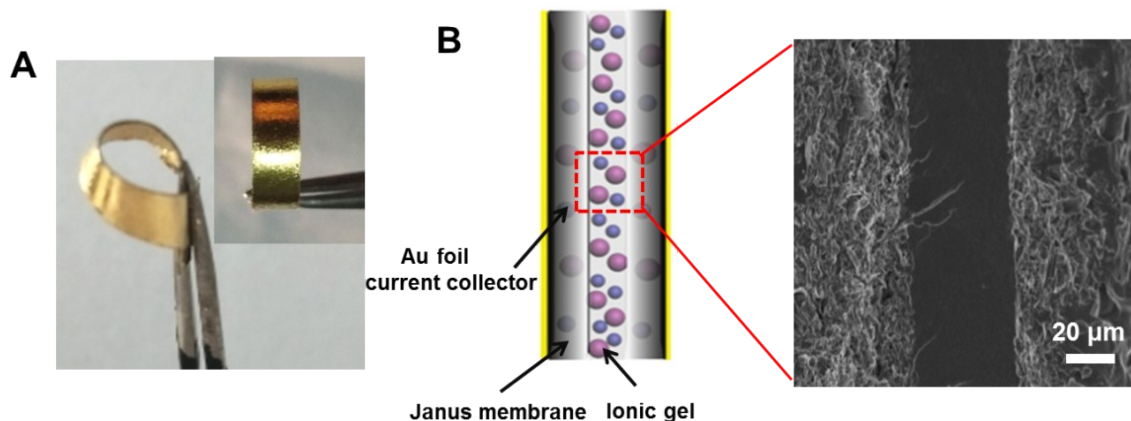
83

84



85

86 **Fig. S14** Optical images of transparent pure ionic gel membrane and its sectional SEM image.

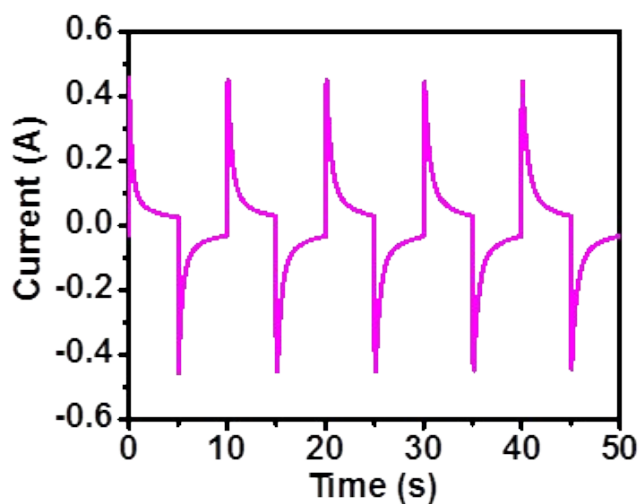


87

88 **Fig. S15** (A) As-fabricated ionic muscle laminated by two 120 nm-thick Au foils as current  
 89 collectors. (B) Schematic structure of the as-fabricated ionic muscle and its cross-sectional  
 90 SEM image.

91

92

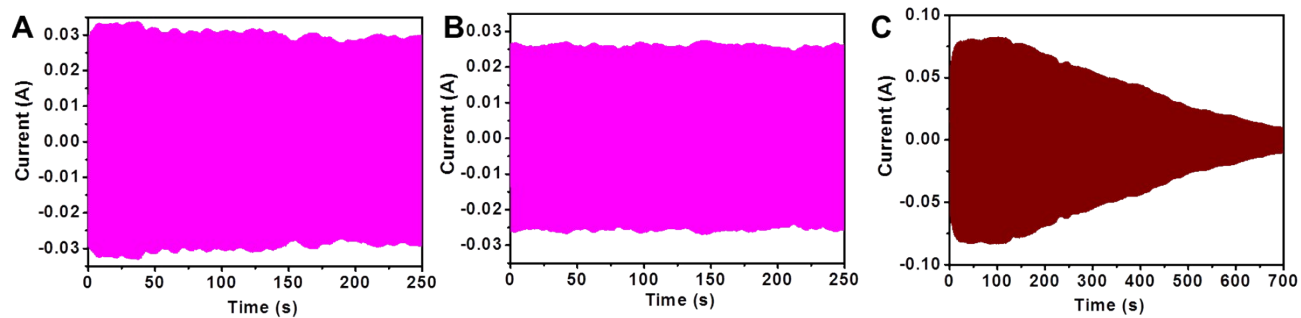


93

94 **Fig. S16** Corresponding current with driving voltage of 3 V and frequency of 0.1 Hz. Power

95 consumption was calculated according to the equation:  $P = \frac{\int_0^T v i dt}{T}$ , where  $p$  is power,  $v$  and  $i$  is

96 the instantaneous voltage and current at time  $t$ , respectively, and  $T$  is the time period.



97

98 **Fig. S17** Cyclic performance of the ionic muscles fabricated with gradient carbon nanomesh

99 electrodes (A & B) and with pure ionic gel electrodes (C). A is for the first 250 cycles, B is

100 for the last 250 cycles (9301<sup>st</sup>–10000<sup>th</sup> cycles), while C is for 700 cycles.

101 **Supporting Videos**

102 **Video S1.** Actuation performance of ionic muscle driven by 3 V at 0.1 Hz.

103 **Video S2.** Temporal actuating behavior of ionic muscle at diverse driving voltages.

104 **Video S3.** Temporal displacement ( $\delta$ ) at 3 V bias with varying frequencies.